Electronic Supplementary Material (ESI) for CrystEngComm.

SUPPORTING INFORMATION

The solvent effect on the structural and magnetic features of bidentate ligand-capped {$Co^{II}_9[W^V(CN)_8]_6$} Single-Molecule Magnets

Szymon Chorazy,[a,b] Anna Hoczek,[a] Maciej Kubicki,[c] Hiroko Tokoro,[b,d] Shin-ichi Ohkoshi,*[b,e]
Barbara Sieklucka,[a] and Robert Podgajny*[a]

[a]*Faculty of Chemistry, Jagiellonian University, Ingardena 3, 30-060 Kraków, Poland. E-mail: robert.podgajny@uj.edu.pl*
[b]*Department of Chemistry, School of Science, The University of Tokyo, 7-3-1 Hongo, Bunkyo-ku,*
113-0033 Tokyo, Japan. E-mail: ohkoshi@chem.s.u-tokyo.ac.jp
[c] *Faculty of Chemistry, Adam Mickiewicz University, Umultowska 89b, 61-614 Poznań, Poland*
[d]*Division of Materials Science, Faculty of Pure and Applied Sciences, University of Tsukuba,*
1-1-1 Tennodai, Tsukuba, Ibaraki 305-8573, Japan
[e]*CREST, JST, K's Gobancho, Chiyoda-ku, Tokyo 102-0076, Japan*

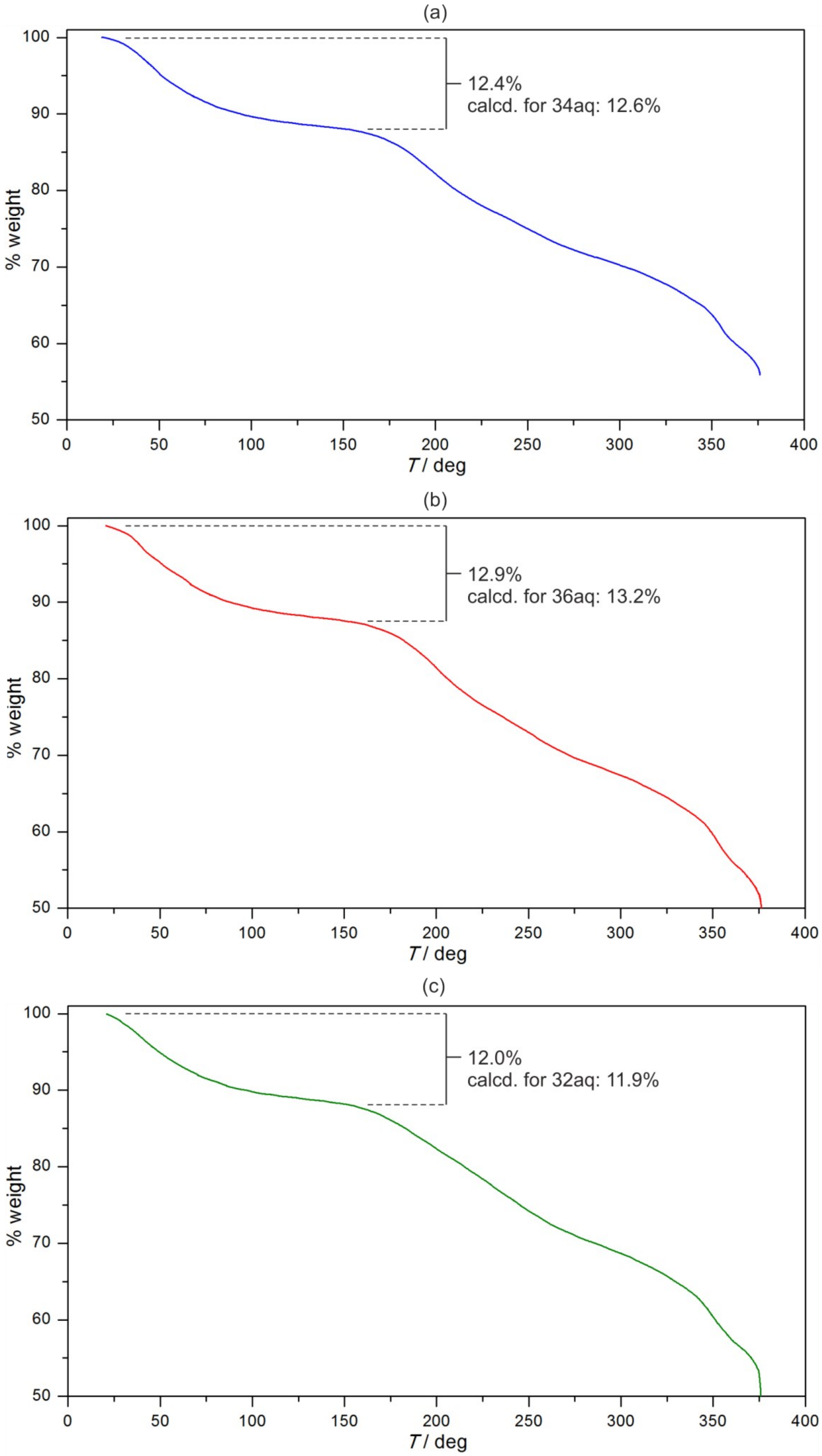

Figure S1 Thermogravimetric curves for hydrated forms of **1** (**1hyd**, *a*), **2** (**2hyd**, *b*), and **3** (**3hyd**, *c*) with the steps related to the loss of solvent molecules of water.

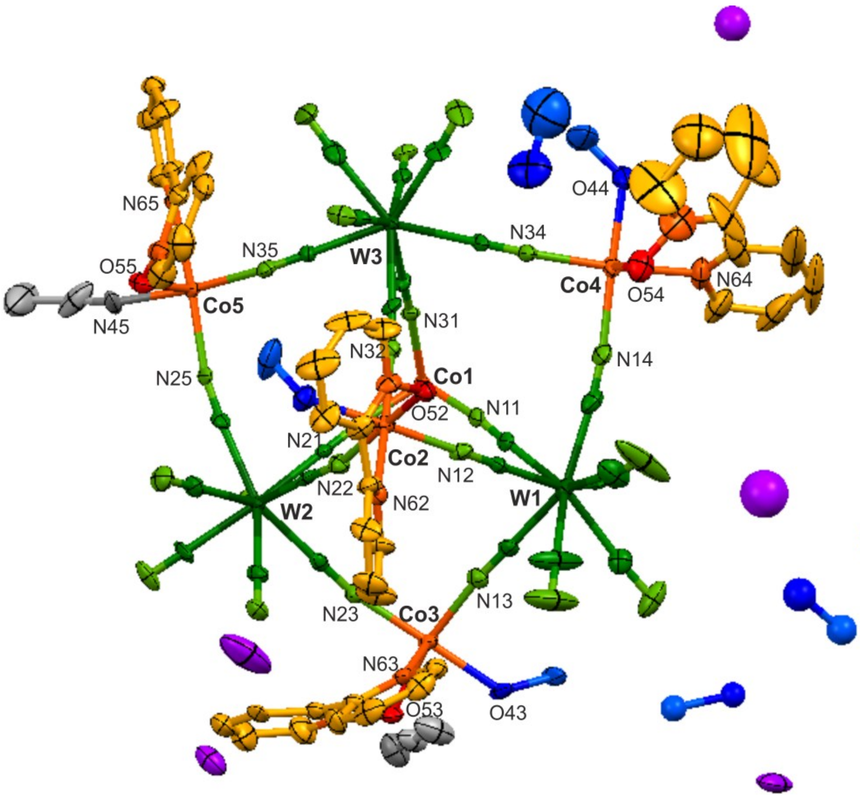

Figure S2 Asymmetric unit of **1** with atom labeling scheme for metal ions and nearest neighbours of Co centers. Atom spheres are shown with 40% probability level. Hydrogen atoms are omitted for clarity. For disordered atoms of terminal cyanides, only one of two possible positions were presented. Colors: Co – orange, W – dark green, cyanides – green, 2,2’-bpmo ligands – light orange and red, methanol – blue, water – violet, acetonitrile – grey.

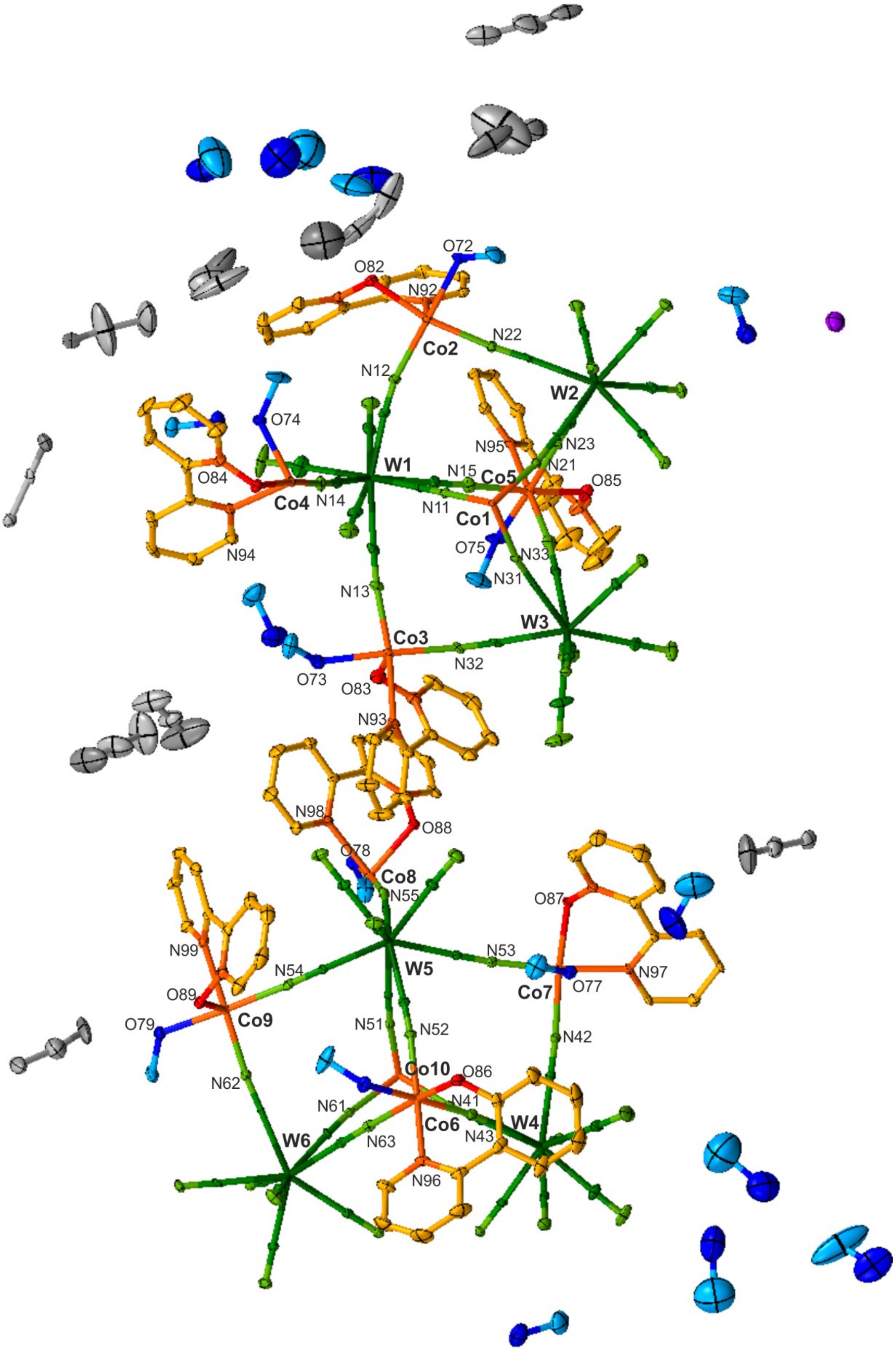

Figure S3 Asymmetric unit of **2** with atom labeling scheme for metal ions and nearest neighbours of Co centers. Atom spheres are shown with 40% probability level. Hydrogen atoms are omitted for clarity. Colors: Co – orange, W – dark green, cyanides – green, 2,2’-bpmo ligands – light orange and red, methanol – blue, water – violet, acetonitrile – grey.

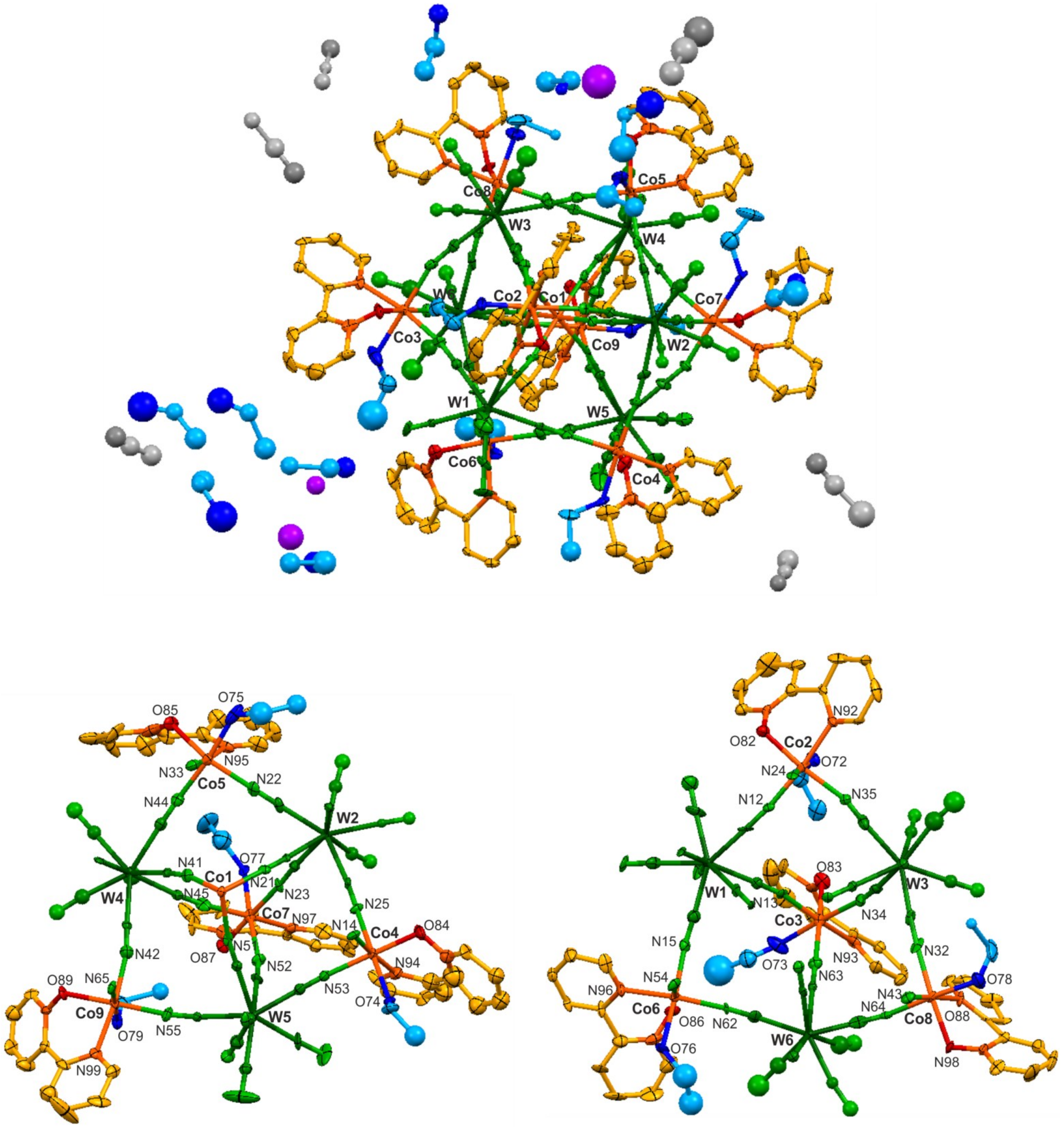

Figure S4 Asymmetric unit of **3** (top) with atom labeling scheme for metal ions, and detailed insight into nearest neighbours of Co centers presented in two separated halves of the asymmetric unit (bottom, left and right). Atom spheres are shown with 40% probability level. Hydrogen atoms are omitted for clarity. Colors: Co – orange, W – dark green, cyanides – green, 2,2'-bpmo ligands – light orange and red, ethanol – blue, water – violet, acetonitrile – grey.

Comment to Figures S2–S4 – Detailed description of asymmetric units of **1**, **2**, and **3**

The asymmetric units are very different in **1**, **2**, and **3** (Figures S2–S4). For **1**, the symmetrically independent unit contains the half of the cluster, comprising 4.5 of Co^{II} centers combined with three $[W^{V}(CN)_8]^{3-}$ complexes, as the second half of the cluster is generated by the inversion centre positioned on the central Co1 (Figure S2). Each tungsten forms five cyanide bridges, while the remaining three cyanide ligands are terminal. The central Co1 coordinates six cyanides by nitrogen atoms. Each of the external Co2, Co3, and Co4 sites coordinate three cyanides in the *fac* configuration, one MeOH molecule by the oxygen atom, and the N,O-bidentate 2,2'-bpmo ligand which results in the overall $\{N_4O_2\}$ coordination. For the Co5 site, MeOH is exchanged by MeCN coordinated by the nitrogen atom, and the $\{N_5O_1\}$ chromophore is thus observed. The asymmetric unit of **1** is completed by the several uncoordinated solvent molecules of H_2O, MeCN, and MeOH.

The asymmetric unit of **2** contains the halves of two clusters, A and B, each of them comprising the $\{Co_{4.5}W_3\}$ unit (Figure S3). The coordination schemes of both types of clusters in **2** are generally analogous as described for **1**. As an only difference, all of the external Co sites in **2** (Co2–Co5 of cluster A, Co7–Co10 of B) coordinate three cyanides, one MeOH molecule, and one 2,2'-bpmo ligand, giving the total $\{N_4O_2\}$ coordination. The cyanido-bridged part of the asymmetric unit in **2** is accompanied by the large amount of uncoordinated solvent molecules of H_2O, MeCN, and MeOH.

Due to the loss of the inversion centre placed in the cluster core, the asymmetric unit of **3** contains two whole cluster accompanied by a number of H_2O, MeCN, and EtOH molecules (Figure S4). The coordination modes of Co and W centers are, however, similar to observed in **2** with EtOH replacing the MeOH molecules. Thus, all of the external Co^{II} sites (Co2–Co9) coordinate three cyanides, one EtOH molecule, and one 2,2'-bpmo ligand, giving the $\{N_4O_2\}$ chromophores.

Table S1 Detailed structure parameters of **1**

Parameter	Value [Å, °]	Parameter	Value [Å, °]
W1 – C	2.10(2) to 2.200(8)	C – N (W1)	1.120(19) to 1.199(8)
W2 – C	2.103(18) to 2.186(16)	C – N (W2)	1.104(19) to 1.175(19)
W3 – C	2.142(19) to 2.185(14)	C – N (W3)	1.111(17) to 1.90(6)
W1 – C - N	175(3) to 179.3(12)	Co1 – N (CN)	2.082(10) 2.089(14) 2.108(11)
W2 – C - N	173.2(12) to 178.8(12)		
W3 – C - N	175(2) to 179.6(14)		
Co2 – N(CN)	2.094(12) 2.098(14) 2.115(12)	Co3 – N(CN)	2.064(14) 2.097(14) 2.108(11)
Co2 – O(MeOH)	2.153(11)	Co3 – O(MeOH)	2.097(14)
Co2 – O(2,2'-bpmo)	2.024(10)	Co3 – O(2,2'-bpmo)	2.039(10)
Co2 – N(2,2'-bpmo)	2.137(13)	Co3 – N(2,2'-bpmo)	2.133(13)
Co4 – N(CN)	2.098(12) 2.100(14) 2.107(14)	Co5 – N(CN)	2.084(12) 2.092(14) 2.124(13)
Co4 – O(MeOH)	2.140(12)	Co5 – N(MeCN)	2.113(15)
Co4 – O(2,2'-bpmo)	2.035(13)	Co5 – O(2,2'-bpmo)	2.050(11)
Co4 – N(2,2'-bpmo)	2.162(15)	Co5 – N(2,2'-bpmo)	2.140(11)
Co1 – N – C (CN)	170.3(11) 172.0(12) 173.9(11)	Co3 – N – C (CN)	163.6(12) 168.6(12) 173.3(13)
Co2 – N – C (CN)	167.9(12) 168.1(11) 171.9(12)	Co4 – N – C (CN)	168.2(13) 168.6(12) 172.7(13)
N – Co1 – N	180, 180, 180 86.6(4), 89.1(4) 88.7(4)	Co5 – N – C (CN)	169.5(11) 170.4(13) 175.2(13)
N(CN) – Co2 – O(N)	171.8(5) 174.1(5) 176.3(5)	N(CN) – Co4 – O(N)	170.3(5) 174.7(6) 178.4(4)
O – Co2 – N (O and N of 2,2'-bpmo)	80.8(5)	O – Co4 – N (O and N of 2,2'-bpmo)	82.0(6)
py – py torsion (2,2'bpmo for Co2)	33.74	py – py torsion (2,2'bpmo for Co4)	33.31
N(CN) – Co3 – O(N)	167.8(5) 171.3(6) 177.6(5)	N(CN) – Co5 – O(N)	168.4(5) 173.3(6) 175.6(4)
O – Co3 – N (O and N of 2,2'-bpmo)	79.8(5)	O – Co5 – N (O and N of 2,2'-bpmo)	80.4(4)
py – py torsion (2,2'bpmo for Co3)	29.43	py – py torsion (2,2'bpmo for Co5)	26.70

Table S2 (part 1) Detailed structure parameters of **2** – cluster A

Parameter	Value [Å, °]	Parameter	Value [Å, °]
W1 – C	2.139(7) to 2.173(5)	C – N (W1)	1.137(7) to 1.175(9)
W2 – C	2.149(4) to 2.189(5)	C – N (W2)	1.143(7) to 1.150(6)
W3 – C	2.157(5) to 2.188(5)	C – N (W3)	1.128(7) to 1.158(8)
W1 – C - N	175.1(4) to 179.1(5)	Co1 – N (CN)	2.082(4) 2.087(4) 2.108(4)
W2 – C - N	174.7(4) to 178.6(4)		
W3 – C - N	173.7(4) to 179.6(8)		
Co2 – N(CN)	2.085(4) 2.113(4) 2.126(4)	Co3 – N(CN)	2.083(4) 2.103(4) 2.112(4)
Co2 – O(MeOH)	2.147(4)	Co3 – O(MeOH)	2.168(4)
Co2 – O(2,2’-bpmo)	2.051(4)	Co3 – O(2,2’-bpmo)	2.037(4)
Co2 – N(2,2’-bpmo)	2.133(4)	Co3 – N(2,2’-bpmo)	2.164(4)
Co4 – N(CN)	2.072(5) 2.102(4) 2.127(4)	Co5 – N(CN)	2.070(5) 2.097(4) 2.101(4)
Co4 – O(MeOH)	2.141(4)	Co5 – O(MeOH)	2.170(4)
Co4 – O(2,2’-bpmo)	2.035(4)	Co5 – O(2,2’-bpmo)	2.025(4)
Co4 – N(2,2’-bpmo)	2.152(4)	Co5 – N(2,2’-bpmo)	2.144(4)
Co1 – N – C (CN)	168.3(4) 170.1(4) 178.1(4)	Co3 – N – C (CN)	172.4(4) 173.4(4) 176.2(4)
Co2 – N – C (CN)	167.3(4) 171.1(4) 174.8(4)	Co4 – N – C (CN)	168.1(4) 172.2(4) 176.1(5)
N – Co1 – N	180, 180, 180 88.39(15), 88.83(15) 88.71(15)	Co5 – N – C (CN)	168.7(4) 172.8(4) 177.5(5)
N(CN) – Co2 – O(N)	167.85(15) 171.94(16) 178.29(15)	N(CN) – Co4 – O(N)	170.13(19) 172.20(17) 178.30(16)
O – Co2 – N (O and N of 2,2’-bpmo)	80.38(15)	O – Co4 – N (O and N of 2,2’-bpmo)	81.21(15)
py – py torsion (2,2’bpmo for Co2)	36.37	py – py torsion (2,2’bpmo for Co4)	32.87
N(CN) – Co3 – O(N)	169.20(17) 173.03(17) 173.07(16)	N(CN) – Co5 – O(N)	174.25(17) 174.45(18) 177.03(18)
O – Co3 – N (O and N of 2,2’-bpmo)	81.55(17)	O – Co5 – N (O and N of 2,2’-bpmo)	82.10(16)
py – py torsion (2,2’bpmo for Co3)	42.61	py – py torsion (2,2’bpmo for Co5)	34.66

Table S2 (part 2) Detailed structure parameters of **2** – cluster B

Parameter	Value [Å, °]	Parameter	Value [Å, °]
W4 – C	2.158(5) to 2.172(5)	C – N (W4)	1.143(6) to 1.157(7)
W5 – C	2.158(5) to 2.179(5)	C – N (W5)	1.137(7) to 1.158(7)
W6 – C	2.155(5) to 2.189(5)	C – N (W6)	1.133(7) to 1.158(7)
W4 – C - N	173.0(4) to 178.2(6)	Co10 – N (CN)	2.085(4) 2.086(4) 2.098(4)
W5 – C - N	174.1(4) to 179.3(5)		
W6 – C - N	175.7(4) to 179.0(4)		
Co6 – N(CN)	2.101(4) 2.111(4) 2.122(4)	Co7 – N(CN)	2.056(4) 2.082(4) 2.118(4)
Co6 – O(MeOH)	2.126(4)	Co7 – O(MeOH)	2.139(4)
Co6 – O(2,2’-bpmo)	2.054(4)	Co7 – O(2,2’-bpmo)	2.048(3)
Co6 – N(2,2’-bpmo)	2.148(4)	Co7 – N(2,2’-bpmo)	2.127(4)
Co8 – N(CN)	2.065(4) 2.084(4) 2.120(4)	Co9 – N(CN)	2.086(4) 2.102(4) 2.120(4)
Co8 – O(MeOH)	2.142(4)	Co9 – O(MeOH)	2.151(4)
Co8 – O(2,2’-bpmo)	2.034(3)	Co9 – O(2,2’-bpmo)	2.048(4)
Co8 – N(2,2’-bpmo)	2.161(4)	Co9 – N(2,2’-bpmo)	2.149(4)
Co10 – N – C (CN)	167.0(4) 169.9(4) 175.0(4)	Co7 – N – C (CN)	166.7(4) 171.7(4) 172.4(4)
Co6 – N – C (CN)	172.2(4) 172.2(4) 173.6(4)	Co8 – N – C (CN)	159.2(4) 166.5(4) 170.9(4)
N – Co10 – N	180, 180, 180 87.05(15), 88.09(15) 89.98(16)	Co9 – N – C (CN)	168.3(4) 170.6(4) 175.4(4)
N(CN) – Co6 – O(N)	169.13(16) 173.43(17) 176.43(16)	N(CN) – Co8 – O(N)	169.81(16) 171.58(16) 174.51(16)
O – Co6 – N (O and N of 2,2’-bpmo)	80.12(16)	O – Co8 – N (O and N of 2,2’-bpmo)	79.66(15)
py – py torsion (2,2’bpmo for Co6)	38.41	py – py torsion (2,2’bpmo for Co8)	35.07
N(CN) – Co7 – O(N)	171.53(17) 174.97(15) 179.56(17)	N(CN) – Co9 – O(N)	168.33(15) 175.21(17) 178.15(16)
O – Co7 – N (O and N of 2,2’-bpmo)	82.34(15)	O – Co9 – N (O and N of 2,2’-bpmo)	80.37(16)
py – py torsion (2,2’bpmo for Co7)	33.93	py – py torsion (2,2’bpmo for Co9)	28.94

Table S3 Detailed structure parameters of **3**

Parameter	Value [Å, °]	Parameter	Value [Å, °]
W1 – C	2.10(3) to 2.29(3)	C – N (W1)	1.02(4) to 1.28(3)
W2 – C	2.10(3) to 2.22(3)	C – N (W2)	1.12(3) to 1.20(3)
W3 – C	2.14(3) to 2.21(5)	C – N (W3)	1.12(3) to 1.18(4)
W4 – C	2.04(4) to 2.22(3)	C – N (W4)	1.11(4) to 1.20(5)
W5 – C	2.12(3) to 2.18(3)	C – N (W5)	1.12(4) to 1.20(4)
W6 – C	2.03(4) to 2.18(3)	C – N (W6)	1.09(4) to 1.28(6)
W1 – C - N	168(3) to 178(3)	W5 – C - N	173(2) to 179(3)
W2 – C - N	169(3) to 179(3)	W6 – C - N	163(4) to 178(3)
W3 – C - N	171(5) to 178(2)	Co1 – N (CN)	2.07(2), 2.08(2), 2.08(3), 2.09(2), 2.10(3), 2.11(2)
W4 – C - N	171(2) to 179(3)		
Co2 – N(CN)	2.06(2), 2.09(3), 2.16(3)	Co3 – N(CN)	2.05(2), 2.07(3), 2.11(3)
Co2 – O(MeOH)	2.11(2)	Co3 – O(MeOH)	2.23(2)
Co2 – O(2,2’-bpmo)	2.05(2)	Co3 – O(2,2’-bpmo)	2.01(2)
Co2 – N(2,2’-bpmo)	2.15(2)	Co3 – N(2,2’-bpmo)	2.15(3)
Co4 – N(CN)	2.08(2), 2.08(3), 2.11(3)	Co5 – N(CN)	2.08(3), 2.11(3), 2.11(3)
Co4 – O(MeOH)	2.12(2)	Co5 – O(MeOH)	2.11(3)
Co4 – O(2,2’-bpmo)	2.02(2)	Co5 – O(2,2’-bpmo)	2.03(2)
Co4 – N(2,2’-bpmo)	2.14(3)	Co5 – N(2,2’-bpmo)	2.09(3)
Co6 – N(CN)	2.03(2), 2.10(3), 2.10(3)	Co7 – N(CN)	2.06(2), 2.09(3), 2.13(2)
Co6 – O(MeOH)	2.13(2)	Co7 – O(MeOH)	2.19(2)
Co6 – O(2,2’-bpmo)	2.07(2)	Co7 – O(2,2’-bpmo)	2.06(2)
Co6 – N(2,2’-bpmo)	2.12(2)	Co7 – N(2,2’-bpmo)	2.12(3)
Co8 – N(CN)	2.05(3), 2.10(3), 2.10(3)	Co9 – N(CN)	2.08(3), 2.09(3), 2.13(2)
Co8 – O(MeOH)	2.11(2)	Co9 – O(MeOH)	2.13(2)
Co8 – O(2,2’-bpmo)	2.06(2)	Co9 – O(2,2’-bpmo)	2.04(2)
Co8 – N(2,2’-bpmo)	2.17(2)	Co9 – N(2,2’-bpmo)	2.13(2)
Co2 – N – C (CN)	163(3), 169(2), 173(2)	Co6 – N – C (CN)	169(2), 173(2), 176(3)
Co3 – N – C (CN)	162(2), 167(2), 176(3)	Co7 – N – C (CN)	161(3), 169(3), 176(2)
Co4 – N – C (CN)	169(2), 174(3), 176(2)	Co8 – N – C (CN)	170(2), 174(3), 177(3)
Co5 – N – C (CN)	159(2), 166(3), 175(2)	Co9 – N – C (CN)	167(3), 167(3), 169(3)
N – Co1 – N	177.6(11), 178.4(11), 178.7(11) N11: 86.4(9), 90.5(8), 91.2(9), 93.1(9)	Co1 – N – C (CN)	165(2), 167(2), 168(2), 168(2), 174(3), 174(3)
N(CN) – Co2 – O(N)	171.4(10), 173.2(9), 178.2(9)	N(CN) – Co4 – O(N)	175.2(11), 175.9(10), 177.1(9)
O – Co2 – N (O and N of 2,2’-bpmo)	81.3(9)	O – Co4 – N (O and N of 2,2’-bpmo)	82.6(11)
py – py torsion (2,2’bpmo for Co2)	35.30	py – py torsion (2,2’bpmo for Co4)	30.22
N(CN) – Co3 – O(N)	167.9(10), 176.6(10), 176.6(11)	N(CN) – Co5 – O(N)	167.6(10), 171.9(10), 173.8(10)
O – Co3 – N (O and N of 2,2’-bpmo)	81.0(10)	O – Co5 – N (O and N of 2,2’-bpmo)	82.2(11)
py – py torsion (2,2’bpmo for Co3)	32.35	py – py torsion (2,2’bpmo for Co5)	38.33
N(CN) – Co6 – O(N)	171.7(10), 175.5(10), 176.7(9)	N(CN) – Co8 – O(N)	170.9(9), 175.1(11), 177.4(11)
O – Co6 – N (O and N of 2,2’-bpmo)	82.6(10)	O – Co8 – N (O and N of 2,2’-bpmo)	81.4(9)
py – py torsion (2,2’bpmo for Co6)	30.16	py – py torsion (2,2’bpmo for Co8)	32.04
N(CN) – Co7 – O(N)	169.9(11), 176.4(9), 176.7(9)	N(CN) – Co9 – O(N)	172.4(11), 177.0(9), 178.4(10)
O – Co7 – N (O and N of 2,2’-bpmo)	82.1(9)	O – Co9 – N (O and N of 2,2’-bpmo)	82.1(9)
py – py torsion (2,2’bpmo for Co7)	31.54	py – py torsion (2,2’bpmo for Co9)	37.52

Table S4 Results of Continuous Shape Measure (CSM) Analysis for $[W^V(CN)_8]^{3-}$ units in **1**, **2**, and **3**

W centre	CSM parameters*			Geometry
	BTP–8	SAPR–8	DD–8	
1				
W1	0.712 (C18A) 1.649 (C18B)	2.272 3.380	2.078 1.242	BTP-8 (C18A) BTP-8/DD-8 (C18B)
W2	2.205	3.027	0.310	DD-8
W3	0.861 (C38A) 1.520 (C38B)	1.655 3.423	0.882 1.656	BTP-8/DD-8
2 - cluster A				
W1	1.739	2.276	0.427	DD-8
W2	1.213	1.666	0.681	DD-8
W3	2.034 (C38A) 0.644 (C38B)	2.673 1.800	0.977 1.748	DD-8 (C38A) BTP-8 (C38B)
2 - cluster B				
W4	1.009	0.961	1.313	BTP-8/SAPR-8
W5	0.965	1.068	1.514	BTP-8/SAPR-8
W6	1.577	2.316	0.436	DD-8
3				
W1	0.817	1.537	1.359	BTP-8
W2	1.389	1.747	0.924	DD-8
W3	1.176	1.477	0.869	DD-8
W4	1.435	1.402	1.364	DD-8/SAPR-8/BTP-8
W5	1.145	1.197	1.182	DD-8/SAPR-8/BTP-8
W6	1.599	2.569	0.748	DD-8

* Continuous Shape Measure (CSM) parameters:[S1,S2]
CSM BTP-8 – the parameter related to the bicapped trigonal prism geometry (C_{2v} symmetry)
CSM SAPR-8 – the parameter related to the square antiprism (D_{4d} symmetry)
CSM DD-8 – the parameter related to the dodecahedron (D_{2d} symmetry)
CSM = 0 for the ideal geometry and increase with the increasing distortion for the ideal polyhedron.

[S1] M. Llunell, D. Casanova, J. Cirera, J. Bofill, P. Alemany, S. Alvarez, M. Pinsky and D. Avnir, *SHAPE v. 2.1. Program for the Calculation of Continuous Shape Measures of Polygonal and Polyhedral Molecular Fragments,* University of Barcelona: Barcelona, Spain, 2013.

[S2] D. Casanova, J. Cirera, M. Llunell, P. Alemany, D. Avnir and S. Alvarez, *J. Am. Chem. Soc.*, 2004, **126**, 1755.

Comment to Table S4 – Detailed analysis of coordination polyhedrons of $[W^V(CN)_8]^{3-}$ units in **1**, **2**, and **3**

The clusters of **1**, **2**, and **3** reveal different detailed structural parameters of $[W^V(CN)_8]^{3-}$ ions, that are bond lengths and angles (Tables S1–S3). It results in the various deformations of the coordination polyhedrons adopted by the flexible W^V complexes which was investigated by means of the Continuous Shape Measure Analysis (Table S4).

In **1**, the perfect dodecahedral (DD-8) geometry can be assigned to W1, while the intermediate geometry between DD-8 and the bicapped trigonal prism (BTP-8) is characteristic of W2 and W3. In the cluster A of **2**, the DD-8 polyhedron can be ascribed both for W1 and W2, while the W3 center reveals the DD-8 or BTP-8 geometry depending on the disordered terminal cyanide described by two positions with 50% occupancies.

The DD-8 geometry is preserved for W6 in the cluster B of **2** but the W5 and W6 sites exhibit different geometry intermediate between the BTP-8, and the square antiprism (SAPR-8) which correlates well with distinct Co-related isomeric forms for this cluster.

The clusters of **3** exhibit a complex scheme of $[W^V(CN)_8]^{3-}$ geometries. However, the domination of DD-8 and BTP-8 is generally observed which is similar to the clusters of **1** and the clusters A in **2** both revealing the identical geometrical isomerism of the cluster as found in **3**. The DD-8 geometry is clearly dominated for W2, W3 and W6 complexes of **3**, while the BTP-8 can be assigned for W1 center. The two remaining W centers, W4 and W5, adopt an intermediate polyhedron between BTP-8, DD-8, and SAPR-8 without the predominant contribution from any of these geometries.

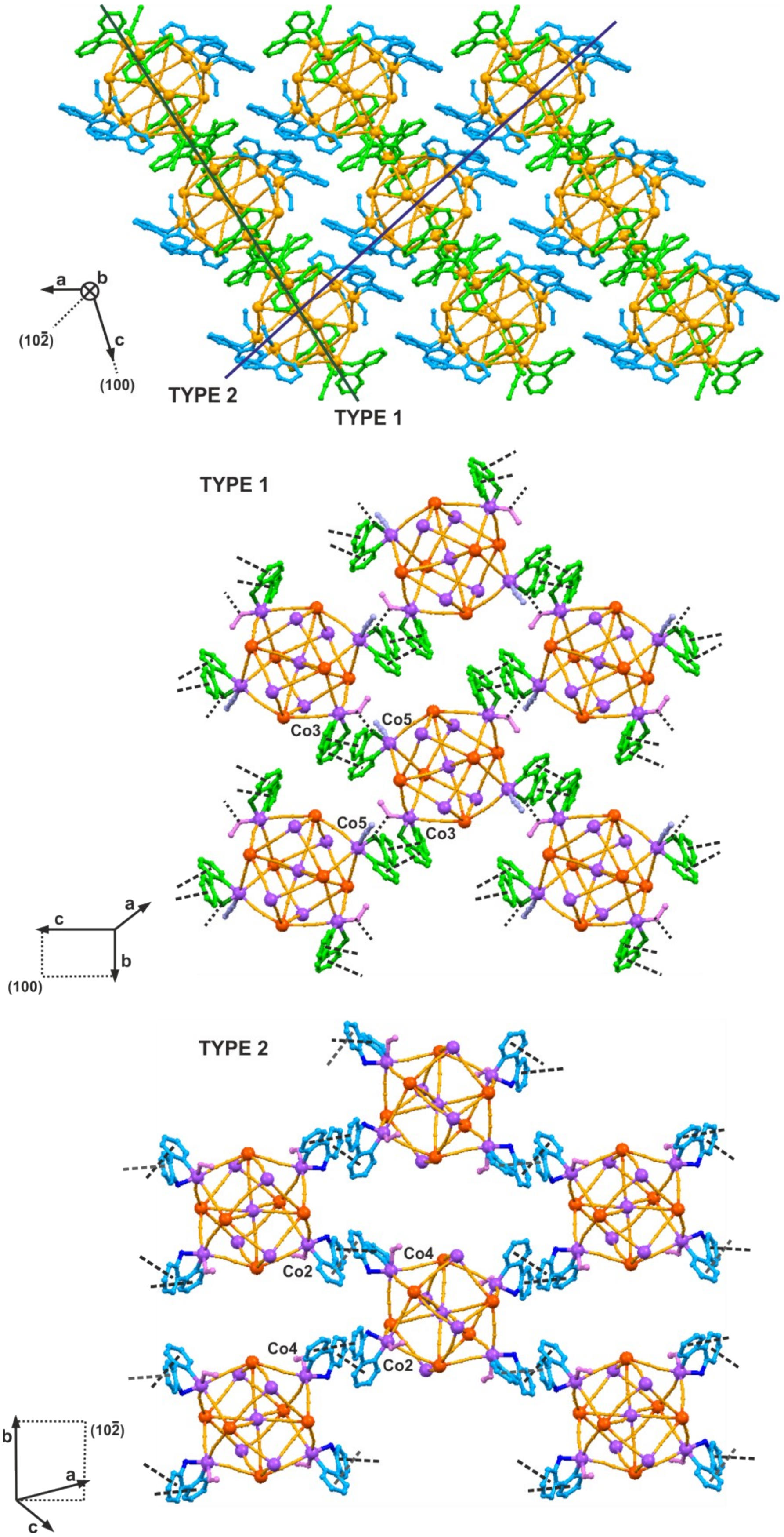

Figure S5. The supramolecular arrangement of $\{Co^{II}_9W^{V}_6\}$ molecules in **1** with the insight into two main types of intercluster contacts within (100) plane (type 1), and (10-2) plane (type 2). Dotted lines correspond to hydrogen bonds and π-π interactions.

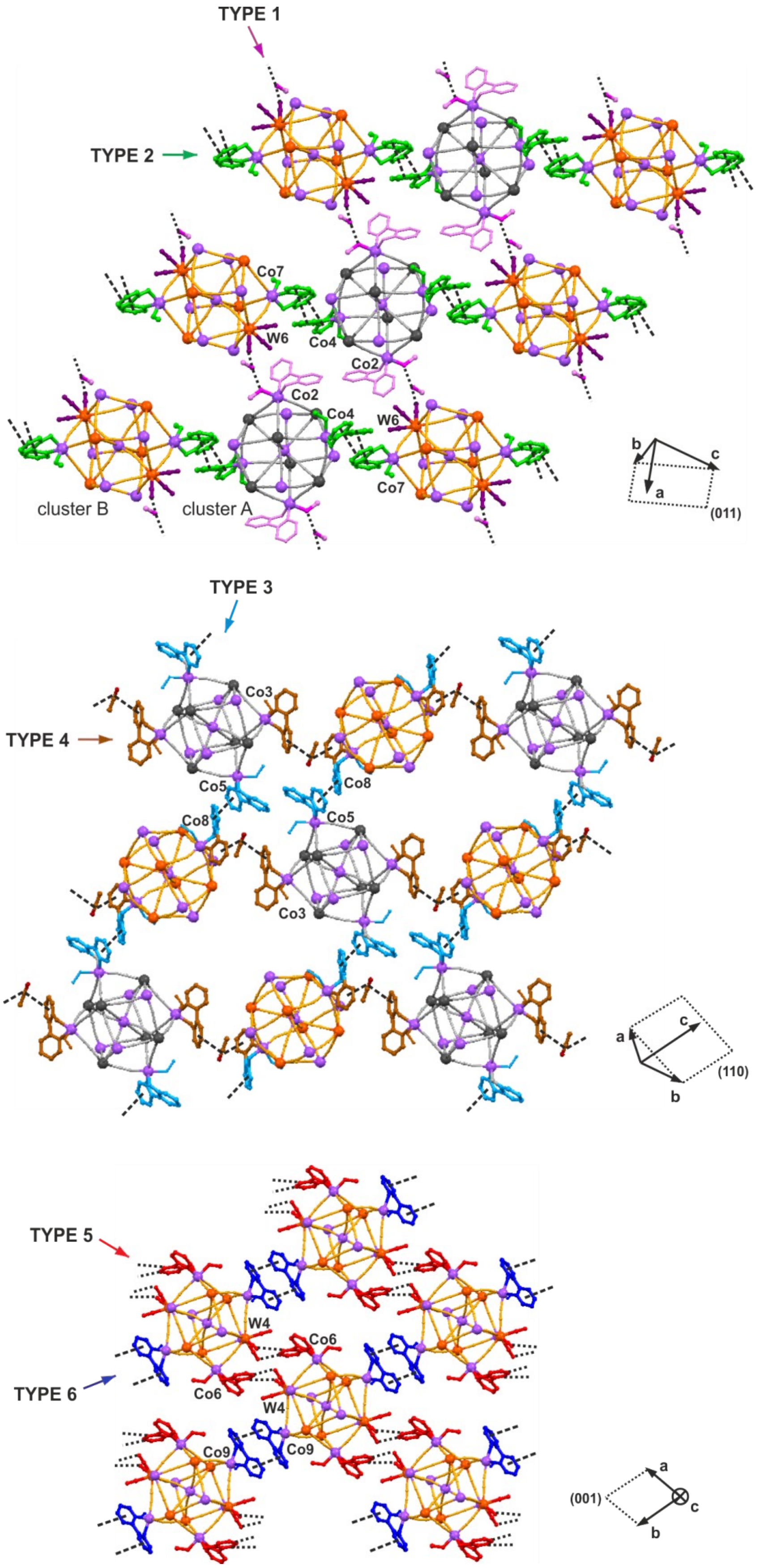

Figure S6. The supramolecular arrangement of $\{Co^{II}_9W^{V}_6\}$ molecules in **2** with the insight into main types of intercluster contacts, within (011) plane (1 and 2), (110) plane (3 and 4), and (001) plane (5 and 6). Dotted lines correspond to hydrogen bonds and π-π interactions. Clusters of A and B types were distinguished by colours.

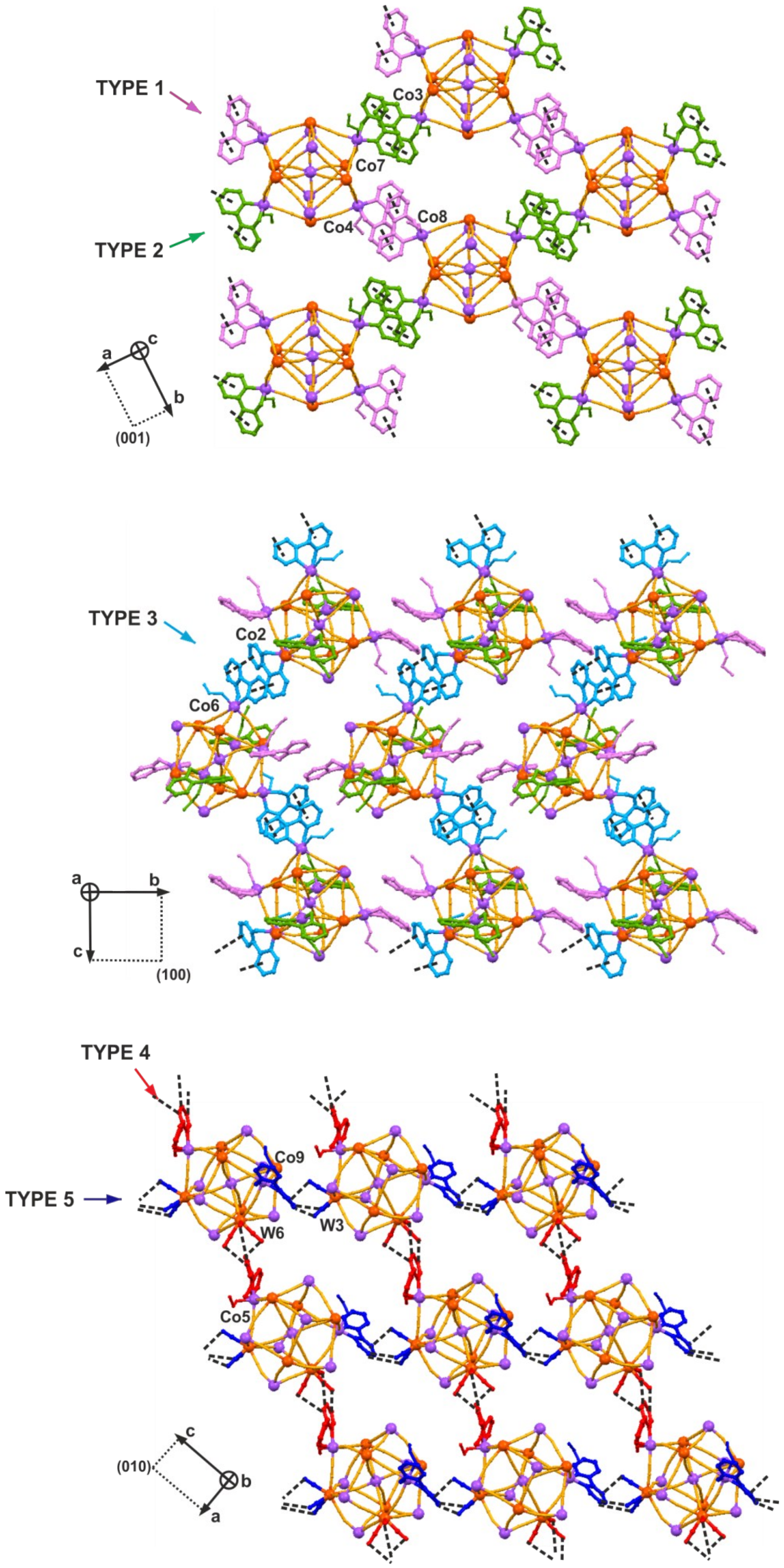

Figure S7. The supramolecular arrangement of $\{\mathrm{Co}^{\mathrm{II}}_{9}\mathrm{W}^{\mathrm{V}}_{6}\}$ molecules in **3** with the insight into main types of intercluster contacts, within (001) plane (types 1 and 2), (100) plane type 3), and (010) plane (types 4 and 5). Dotted lines correspond to hydrogen bonds and π-π interactions.

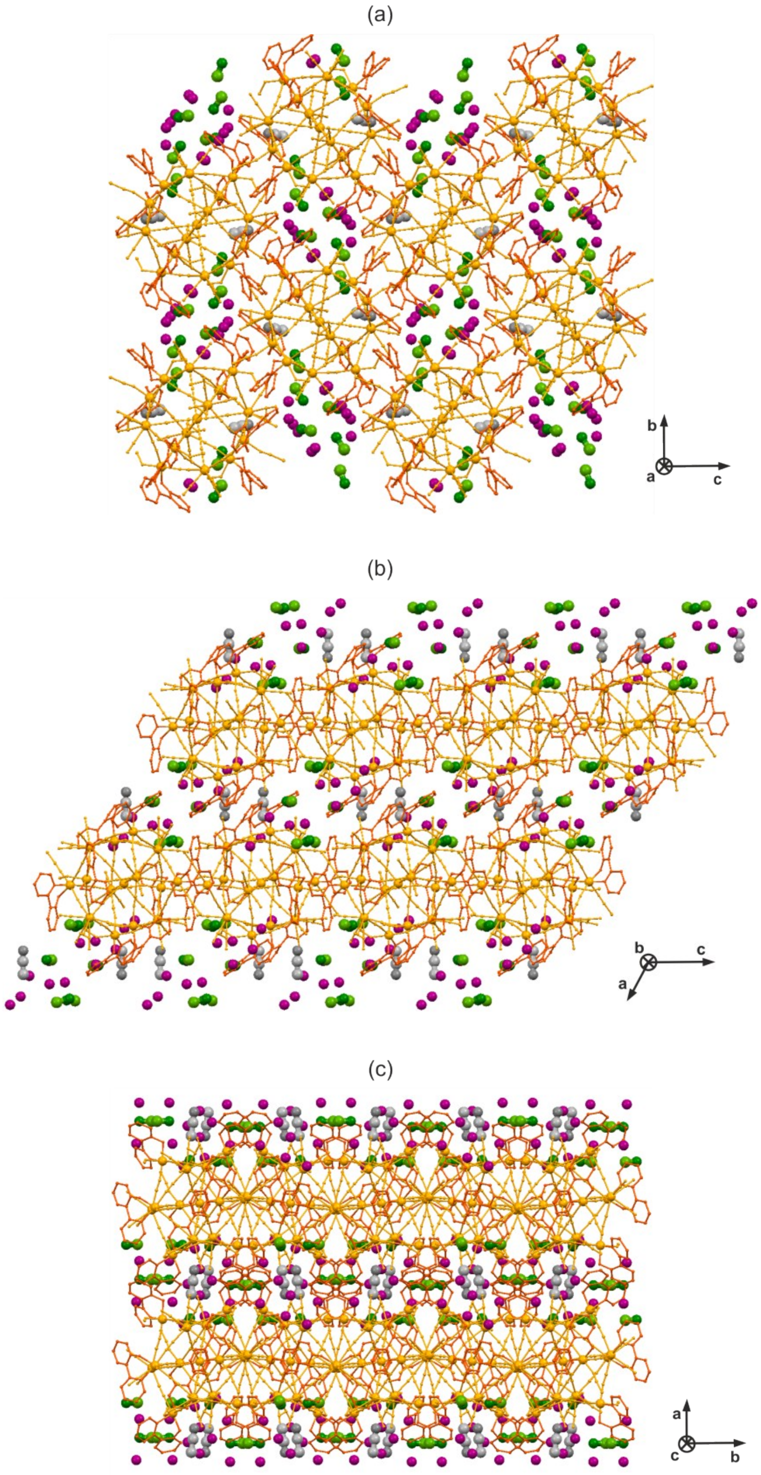

Figure S8 The supramolecular arrangement of cyanido-bridged clusters (orange) and crystallization solvent molecules of water (purple), methanol (green) and acetonitrile (grey) in the crystal structure of **1** presented in the views along **a**, **b**, and **c** crystallographic directions (a, b, c, respectively). Hydrogen atoms are omitted for clarity.

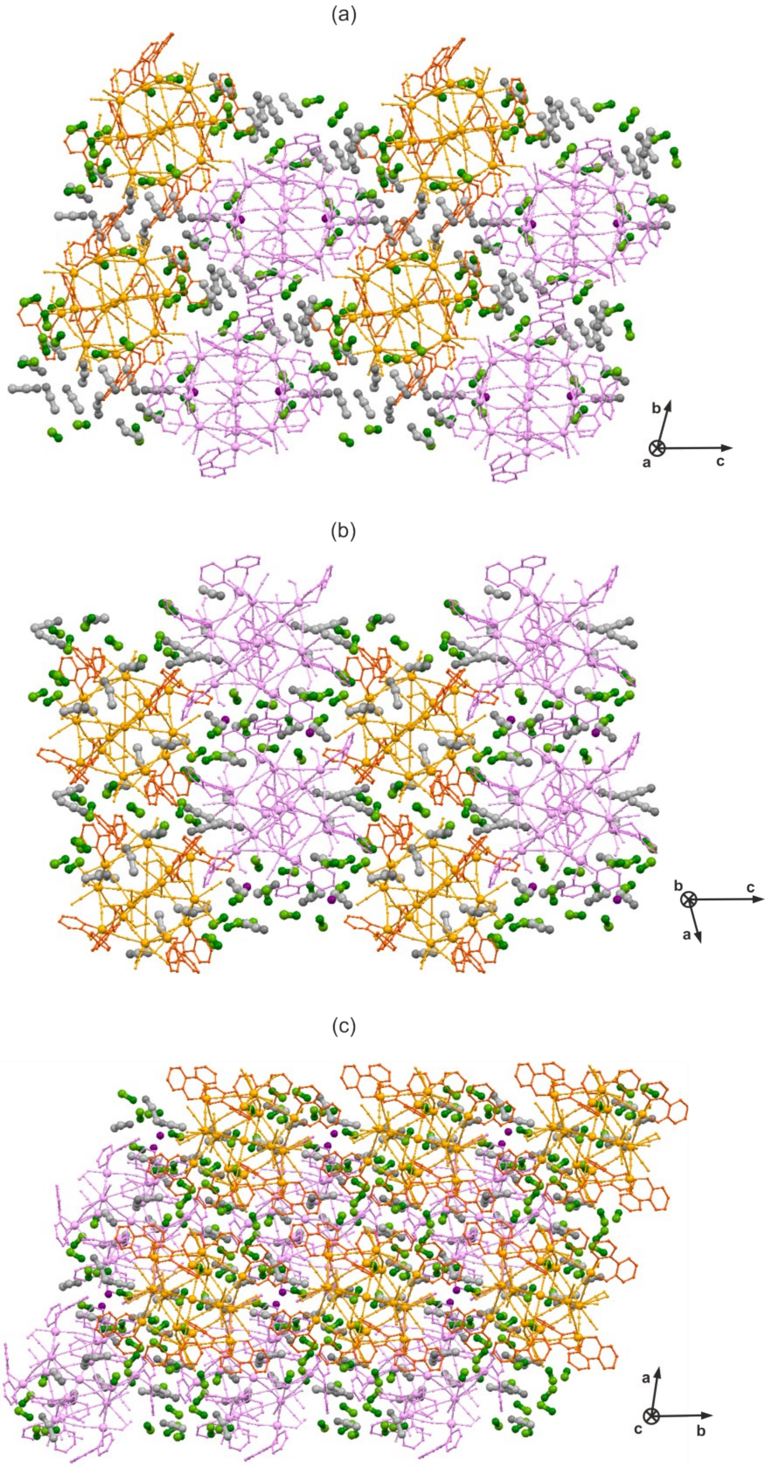

Figure S9 The supramolecular arrangement of cyanido-bridged clusters and crystallization solvent molecules of water (purple), methanol (green) and acetonitrile (grey) in the crystal structure of **2** presented in the views along **a**, **b**, and **c** crystallographic directions (a, b, c, respectively). The two types of cyanido-bridged clusters are distinguished by colors: orange for cluster A, light violet for cluster B. Hydrogen atoms are omitted for clarity.

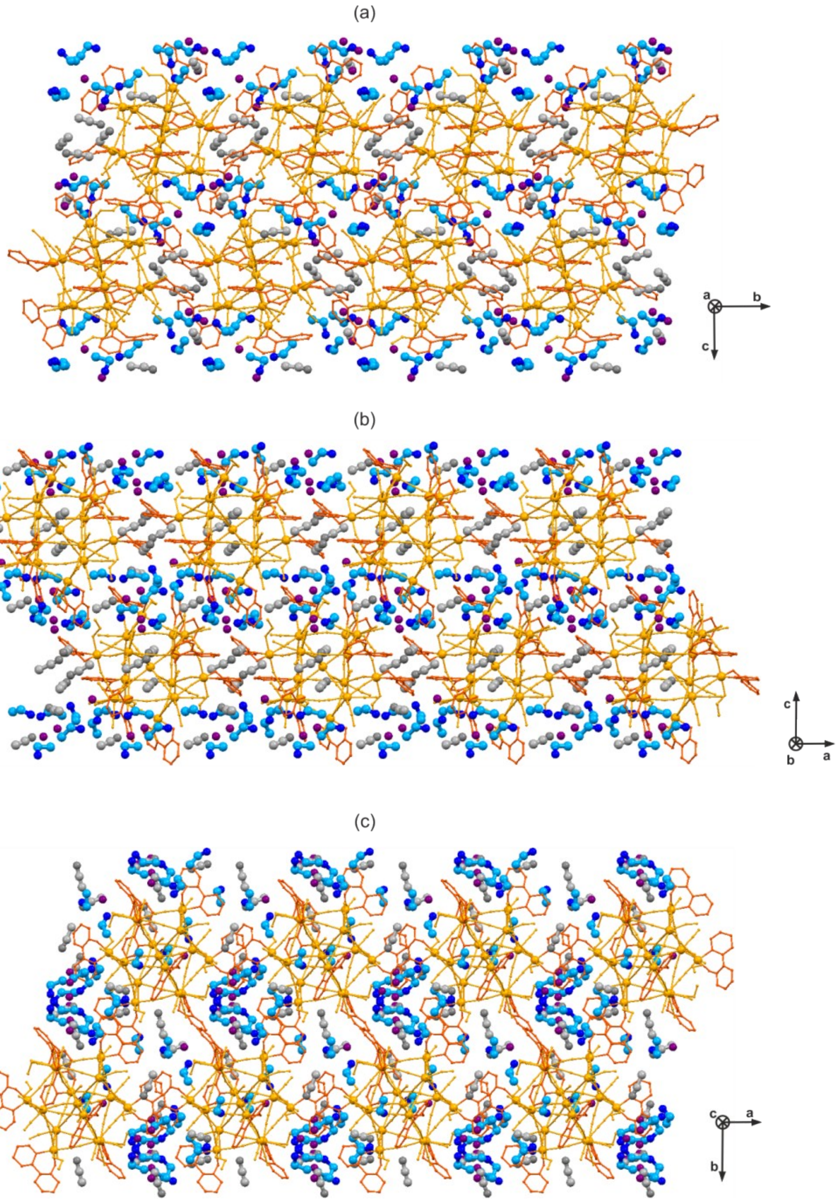

Figure S10 The supramolecular arrangement of cyanido-bridged clusters and crystallization solvent molecules of water (purple), ethanol (blue) and acetonitrile (grey) in the crystal structure of **3** presented in the views along **a**, **b**, and **c** crystallographic directions (a, b, c, respectively). Hydrogen atoms are omitted for clarity.

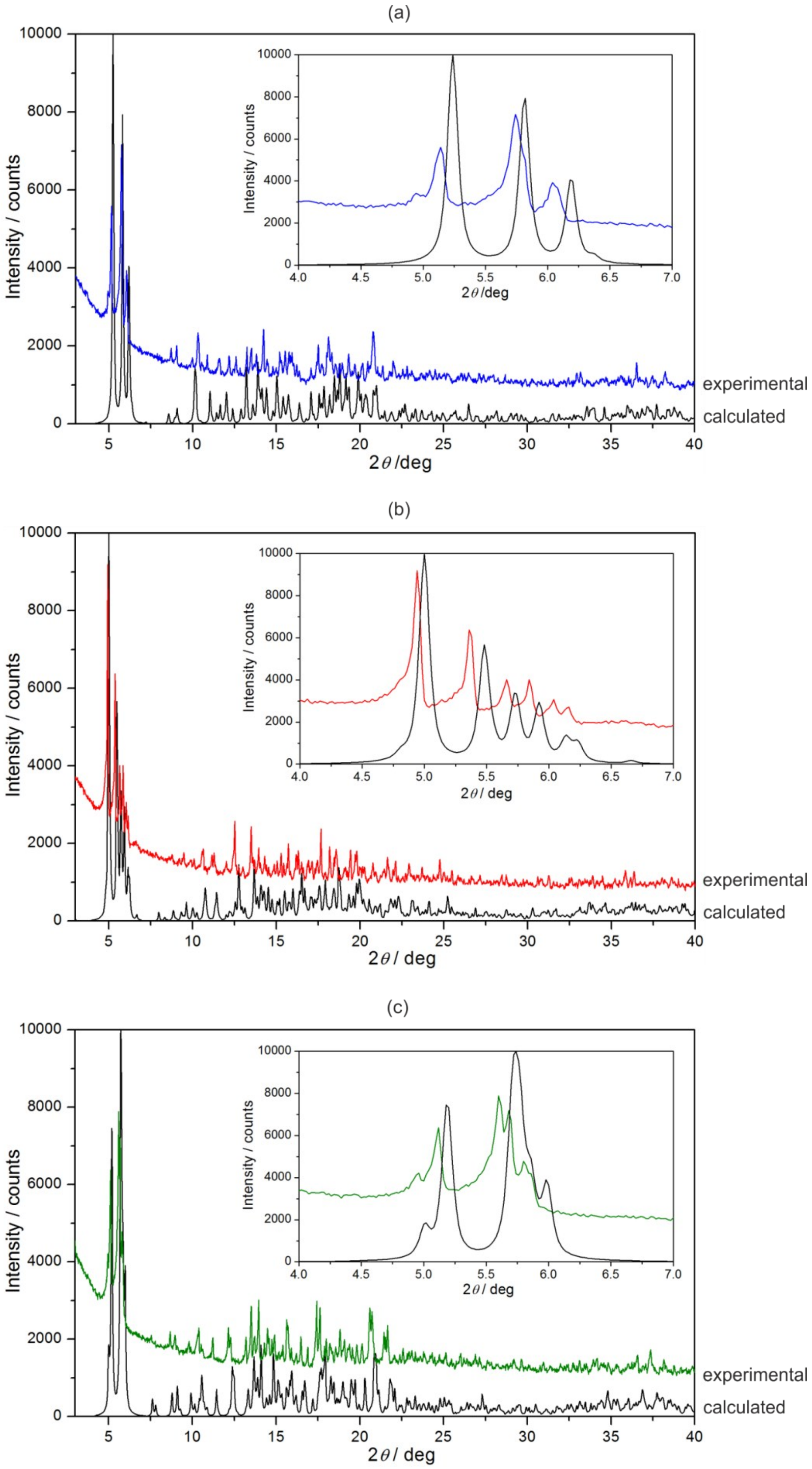

Figure S11 Experimental and calculated (from the single crystal X-ray model) powder X-ray diffraction patterns of **1**(*a*), **2** (*b*), and **3** (*c*) in the representative 3–40° range of 2*Θ* angle. The low-angle range of 4–7° was additionally presented in the inset. The consequent shift of all peaks between the experimental and the calculated patterns is due to the standard temperature effect, as the PXRD experiment was performed at room temperature, while the single-crystal X-ray measurement was done at low temperature of 100 K.

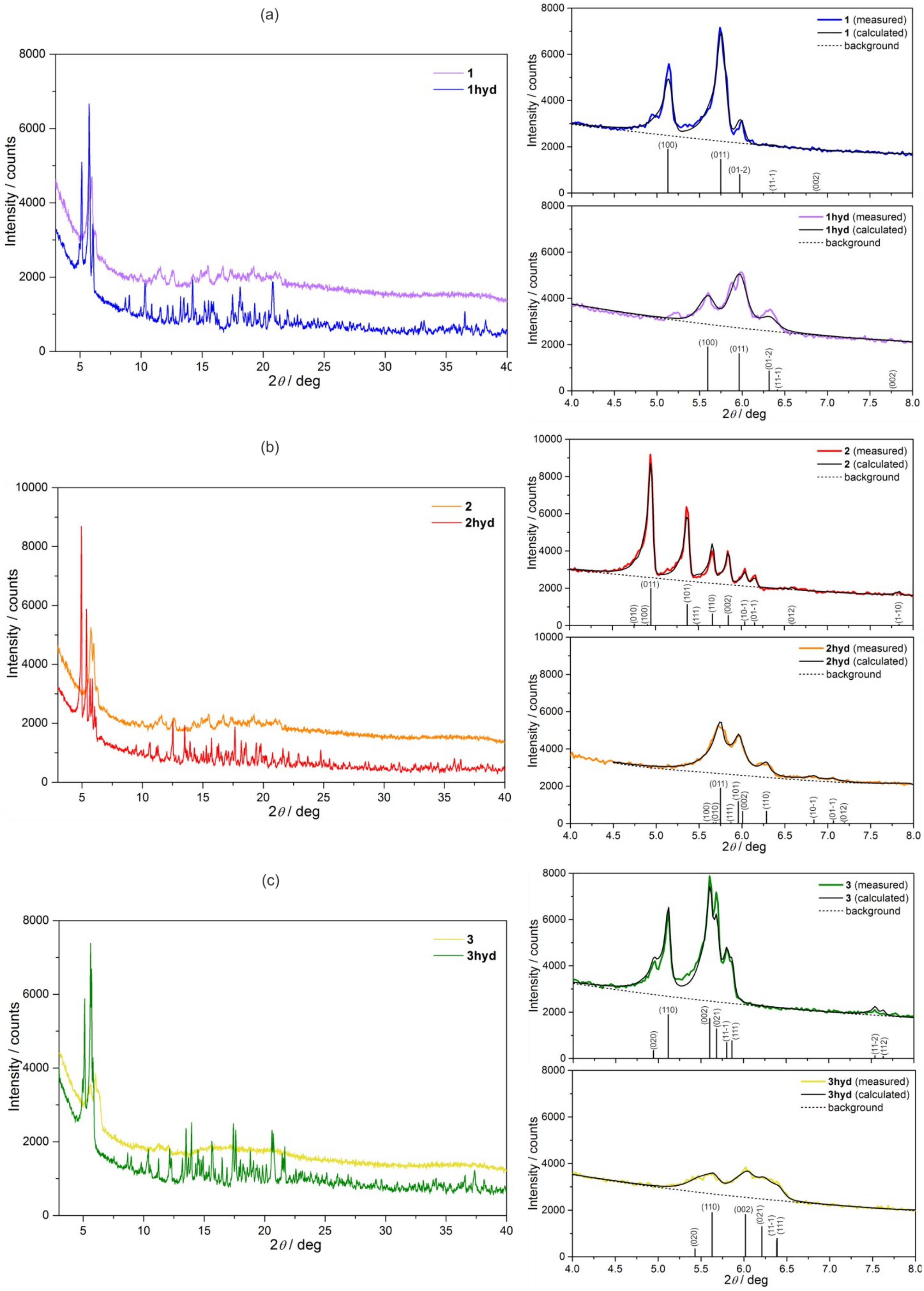

Figure S12 Powder X-ray diffraction patterns at T = 298 K for as synthesized and hydrated (**hyd**) forms of **1** (*a*), **2** (*b*), and **3** (*c*) and the results of cell parameters fittings (right column) based on the 2Θ ranges of 4-8°. The unit cell parameters from the single-crystal XRD studies (T = 100 K) were used as the starting values, and the Rietveld analysis without changing the space group and positions of the atoms was done. For clear comparison in the left colum, the diffraction intensities for as synthesized compounds, **1**–**3** were lowered by the value of 500 counts.

Table S5 Summary of unit cell parameters for **1**, **2**, **3**, and their hydrated forms (**1hyd**, **2hyd**, **3hyd**)

Phase	*T* [K]	Space group	***a*** [Å]	***b*** [Å]	***c*** [Å]	α [deg]	β [deg]	γ [deg]	***V* [Å³]**	method
1	100(1)	$P2_1$/c	20.2531(7)	19.4998(4)	29.3833(8)	90	122.990(3)	90	**9733.4(5)**	single crystal XRD
1	298(2)		20.4(1)	19.16(9)	30.50(10)	90	122.5(5)	90	**10050(79)**	powder XRD
1hyd	298(2)		19.64(2)	19.5(3)	28.31(2)	90	126.44(6)	90	**8709(154)**	powder XRD
2	100(2)	*P*-1	19.0923(3)	20.3195(4)	31.5482(6)	72.427(1)	77.063(1)	68.621(1)	**10775.3(4)**	single crystal XRD
2	298(2)		19.450(7)	20.502(7)	31.953(16)	72.54(7)	76.93(6)	68.94(6)	**11242(8)**	powder XRD
2hyd	298(2)		17.69(2)	17.90(2)	31.71(7)	70.0(3)	73.0(2)	63.4(2)	**8315(24)**	powder XRD
3	100(2)	*C*c	19.4379(4)	35.2593(9)	30.9195(6)	90	91.670(6)	90	**21182.2(8)**	single crystal XRD
3	298(2)		19.717(8)	35.73(2)	31.522(11)	90	90.83	90	**22203(17)**	powder XRD
3hyd	298(2)		17.908(19)	32.53(4)	29.36(2)	90	90.0(19)	90	**17102(32)**	powder XRD

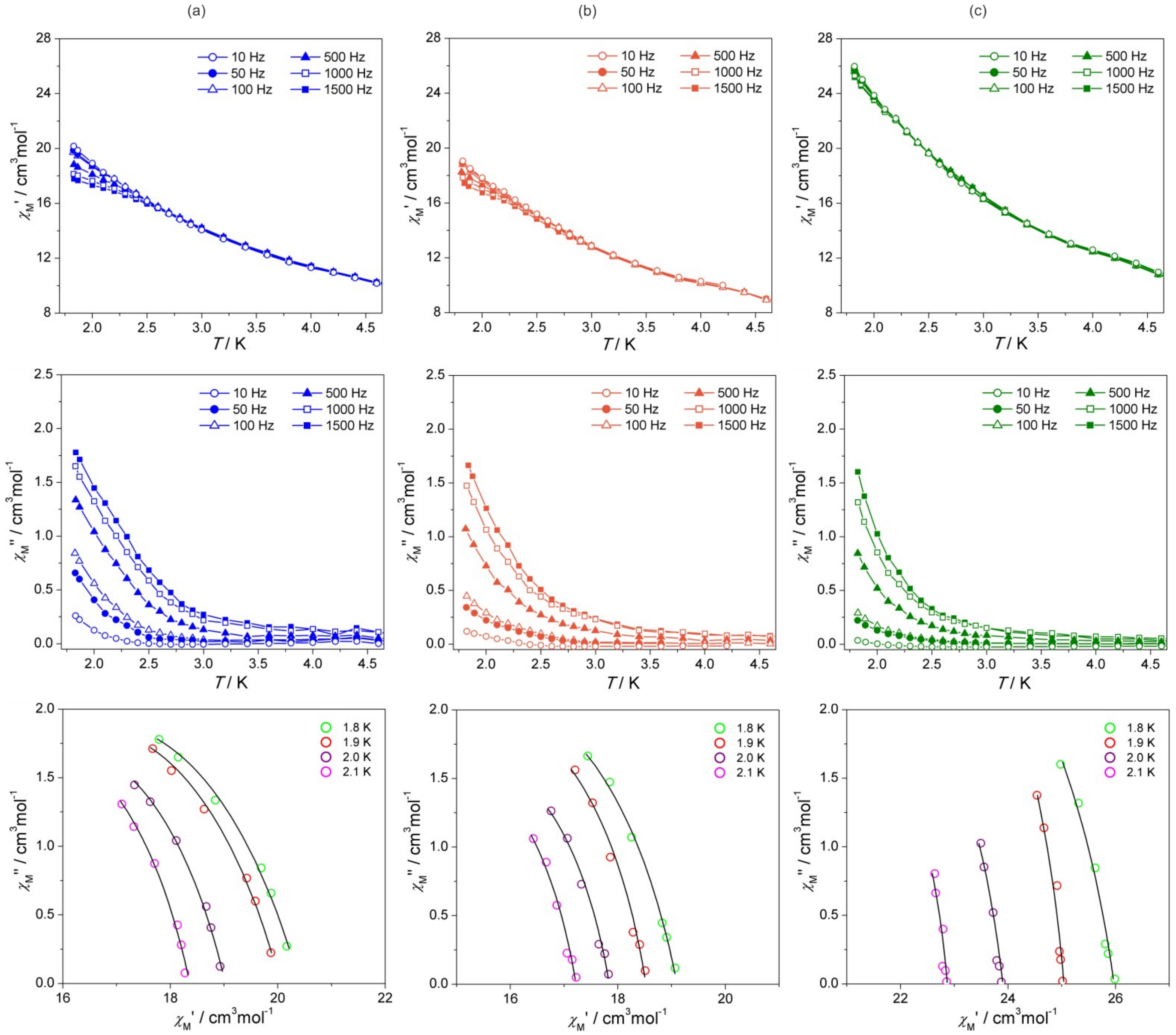

Figure S13 Temperature dependences of *ac* magnetic susceptibility of **1** (a), **2** (b), and **3** (c): χ_M' versus T plots (top), χ_M" versus T plots (middle), and the corresponding χ_M" versus χ_M' Cole – Cole plots at four different temperatures (bottom). The solid lines in the Cole – Cole plots correspond to the fit of the data to a generalized Debye model.[S3,S4] Experimental conditions: H_{dc} = 0 Oe, H_{ac} = 3 Oe. The best fits of the Cole – Cole plots result in the following average α parameters: α(**1**) = 0.35(5), α(**2**) = 0.26(4), and α(**3**) = 0.17(4).

[S3] K. S. Cole and R. H. Cole, *J. Chem. Phys.*, 1941, **9**, 341.

[S4] S. Chorazy, M. Reczyński, R. Podgajny, W. Nogaś, S. Buda, M. Rams, W. Nitek, B. Nowicka, J. Mlynarski, S. Ohkoshi, B. Sieklucka, *Cryst. Growth Des.*, 2015, **15**, 3573.

Comment to Figures 5 and S13 – Determination of ΔE and τ_0 from $ln(\chi''/\chi')(T^{-1})$ plots[S4]

For the determination of ΔE and τ_0 the general formula was used:

$$\tau = \tau_0 exp(\Delta E/k_B T)$$

The χ_0 was reasonably neglected in the Cole-Cole method:

$$\frac{\chi''}{\chi'} = \frac{(\omega\tau)^{1-\alpha}cos(\alpha\pi/2)}{1 + (\omega\tau)^{1-\alpha}sin(\alpha\pi/2)}$$

For $\omega\tau \ll 1$, which is far above the maximum in $\chi''(T)$, we obtained:

$$ln\frac{\chi''}{\chi'} \approx \ln cos\frac{\alpha\pi}{2} + (1-\alpha)\ln\left(\omega\tau_0\right) + (1-\alpha)\frac{\Delta E}{k_B T}$$

The fitted line $ln(\chi''/\chi')(T^{-1})$ cross the vertical axis in:

$$\ln\cos\frac{\alpha\pi}{2} + (1-\alpha)ln(\omega\tau_0)$$

which allows to calculate τ_0 assuming $\omega = 2\pi f$.

Using the α parameters obtained from the best fits of the Cole – Cole plots (Figure S13), and the parameters of the linear fitting to the $ln(\chi''/\chi')(T^{-1})$ plots (Figure 5), the following values of ΔE and τ_0 were obtained:

(a) compound **1**: $\Delta E/k_B$ = 11(2) K; τ_0 = 3.6(12)·10^{-8} s
(b) compound **2**: $\Delta E/k_B$ = 10.1(11) K; τ_0 = 3.3(9)·10^{-8} s
(c) compound **3**: $\Delta E/k_B$ = 10.7(14) K; τ_0 = 1.7(6)·10^{-8} s.

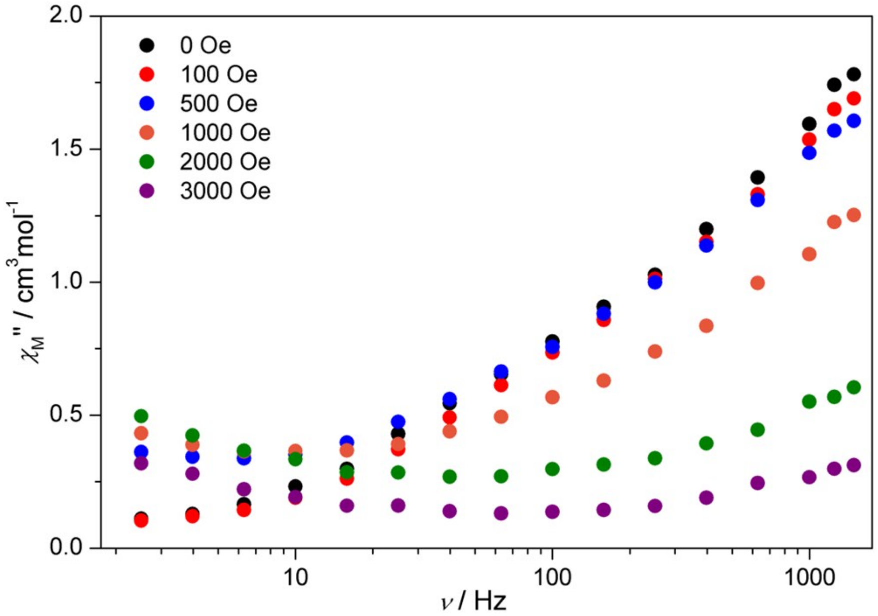

Figure S14 Frequency dependences of out-of-plane *ac* magnetic susceptibility of **1** at various indicated *dc* magnetic fields from the 0 – 3000 Oe range (H_{dc} = 0, 100, 500, 1000, 2000, 3000 Oe; H_{ac} = 3 Oe). The analogous featureless χ_M" versus ν curves at various *dc* magnetic fields were found also for **2** and **3** (not shown) suggesting that the application of external *dc* field does not improve the *ac* magnetic characteristics for $\{Co^{II}_9W^V_6\}$ clusters, as was also reported for other compounds from this family.[S4,S5]

[S5] S. Chorazy, R. Podgajny, W. Nitek, M. Rams, W. Nitek, S. Ohkoshi, B. Sieklucka, *Cryst. Growth Des*., 2013, **13**, 3036.